



# Detector concepts/requirements for a Muon Collider

Massimo Casarsa

*INFN-Trieste, Italy*

**on behalf of the Muon Collider International Collaboration**



G.A. No. 101094300 and 101004730

*L'INFN e la Strategia Europea per la Fisica delle Particelle  
Rome, Italy, May 6-7 2024*

- The **requirements** for the detector specifications **from physics** are similar to those of other multi-TeV machines to reconstruct:
  - ▶ boosted low- $p_T$  physics objects from Standard Model processes;
  - ▶ central energetic physics objects from decays of possible new massive states;
  - ▶ less conventional experimental signatures: disappearing tracks, displaced leptons, displaced photons or jets, ...
- **Constraints from the machine** design: final focusing quadrupoles at  $\pm 6$  m from the interaction point.
- **Machine background** conditions.

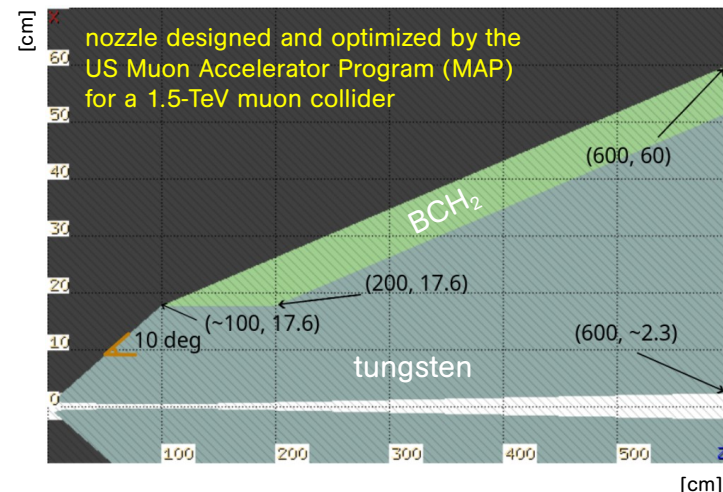
Ultimately, the detector design, the technological choices, and the development of the event reconstruction algorithms will be driven by the high levels of machine-induced background.

	Description	Relevance as background
<b>Muon decay</b>	Decay of stored muons around the collider ring	<b>Dominating source</b>
<b>Synchrotron radiation by stored muons</b>	Synchrotron radiation emission by the beams in magnets near the IP (including IR quads → large transverse beam tails)	<b>Small</b>
<b>Muon beam losses on the aperture</b>	Halo losses on the machine aperture, can have multiple sources, e.g.: <ul style="list-style-type: none"> <li>• Beam instabilities</li> <li>• Machine imperfections (e.g. magnet misalignment)               <ul style="list-style-type: none"> <li>• Elastic (Bhabha) <math>\mu\mu</math> scattering</li> </ul> </li> <li>• Beam-gas scattering (Coulomb scattering or Bremsstrahlung emission)               <ul style="list-style-type: none"> <li>• Beamstrahlung (deflection of muon in field of opposite bunch)</li> </ul> </li> </ul>	<b>Can be significant</b> (although some of the listed source terms are expected to yield a small contribution like elastic $\mu\mu$ scattering, beam-gas, Beamstrahlung)
<b>Coherent <math>e^-e^+</math> pair production</b>	Pair creation by real* or virtual photons of the field of the counter-rotating bunch	<b>Expected to be small</b> (but should nevertheless be quantified)
<b>Incoherent <math>e^-e^+</math> pair production</b>	Pair creation through the collision of two real* or virtual photons emitted by muons of counter-rotating bunches	<b>Significant</b>

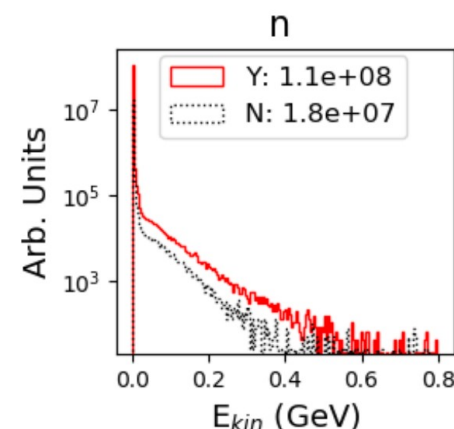
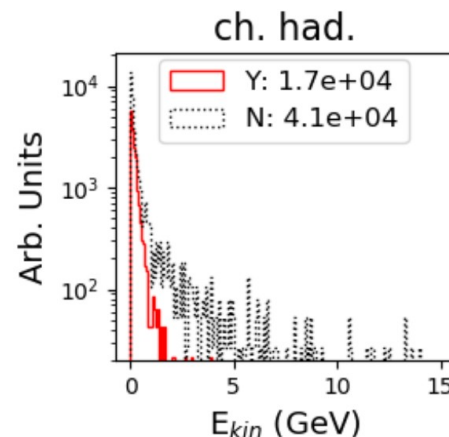
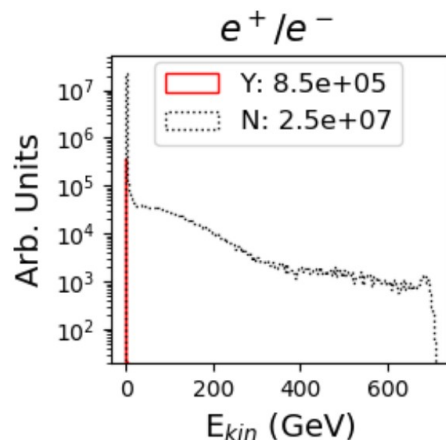
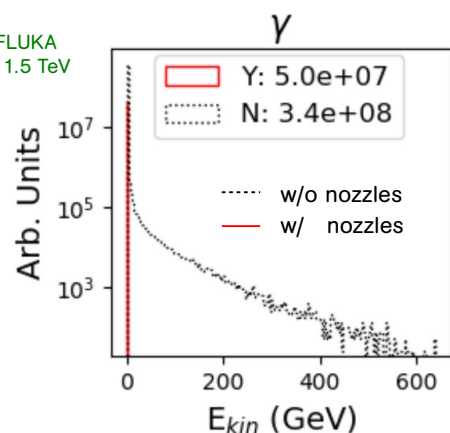
from yesterday's presentation by D. Calzolari

- The detector studies presented here take into account only the dominant background from muon decays  
→ **beam-induced background (BIB)**.

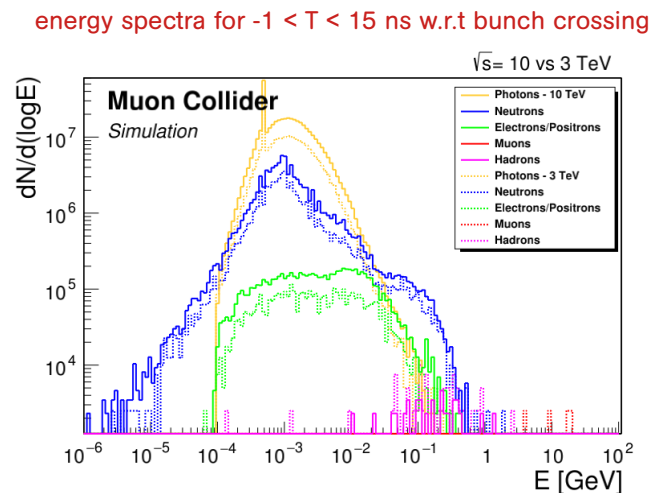
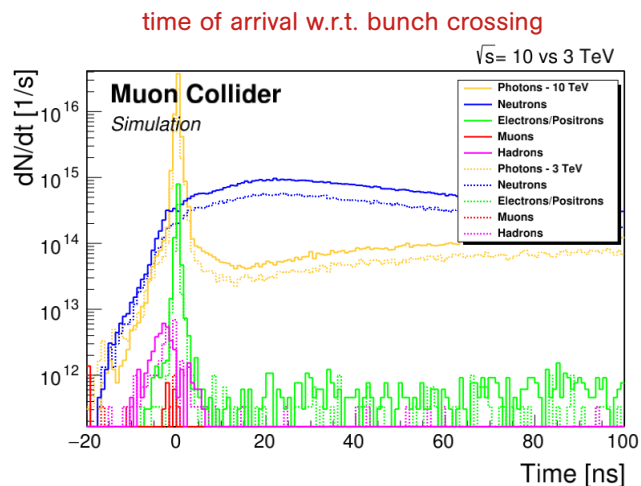
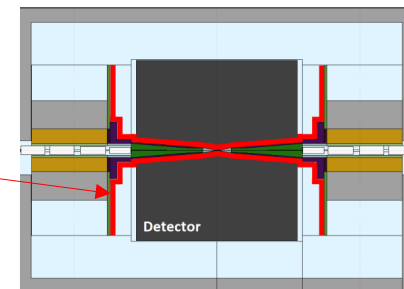
- The machine-detector interface (MDI) includes two conical tungsten shields (“nozzles”) coated with borated polyethylene:
  - ▶ in combination with an appropriate configuration of the interaction region magnets, the nozzles **significantly reduce the background particle flux** into the detector.



FLUKA  
@ 1.5 TeV



- The BIB samples are generated with **FLUKA**, which transports the background particles up to the detector envelope  
→ details in D. Calzolari's presentation.
- On average,  $\sim 10^8$  BIB particles enter the detector volume at every bunch crossing:  
mostly photons, neutrons, electrons/positrons, and charged hadrons.



- For the time being, using the **same 1.5-TeV nozzles** for both 3 and 10 TeV samples  
→ beam-induced background characteristics in the detector mainly determined by the nozzles.

# Detector concept for $\sqrt{s} = 3 \text{ TeV}$

## hadronic calorimeter

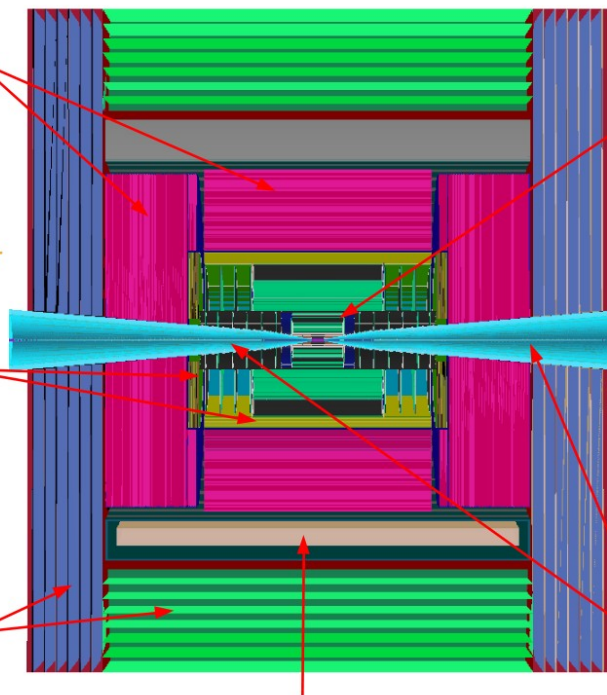
- ◆ 60 layers of 19-mm steel absorber + plastic scintillating tiles;
- ◆ 30x30 mm<sup>2</sup> cell size;
- ◆ 7.5  $\lambda_I$ .

## electromagnetic calorimeter

- ◆ 40 layers of 1.9-mm W absorber + silicon pad sensors;
- ◆ 5x5 mm<sup>2</sup> cell granularity;
- ◆ 22  $X_0 + 1 \lambda_I$ .

## muon detectors

- ◆ 7-barrel, 6-endcap RPC layers interleaved in the magnet's iron yoke;
- ◆ 30x30 mm<sup>2</sup> cell size.



superconducting solenoid (3.57T)

## tracking system

- ◆ **Vertex Detector:**
  - double-sensor layers (4 barrel cylinders and 4+4 endcap disks);
  - 25x25  $\mu\text{m}^2$  pixel Si sensors.
- ◆ **Inner Tracker:**
  - 3 barrel layers and 7+7 endcap disks;
  - 50  $\mu\text{m} \times 1 \text{ mm}$  macro-pixel Si sensors.
- ◆ **Outer Tracker:**
  - 3 barrel layers and 4+4 endcap disks;
  - 50  $\mu\text{m} \times 10 \text{ mm}$  micro-strip Si sensors.

## shielding nozzles

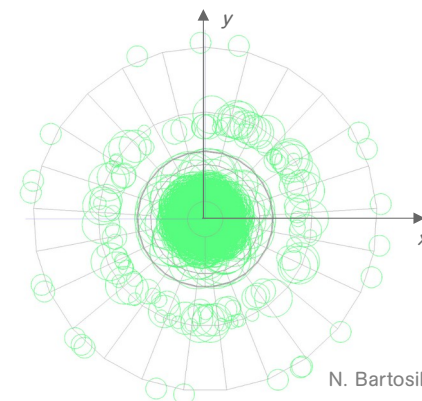
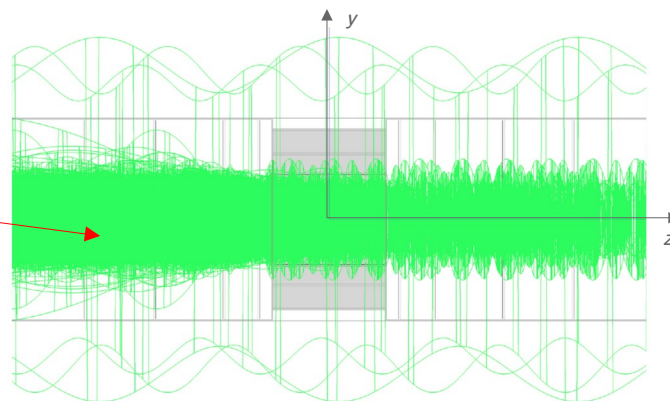
- ◆ Tungsten cones + borated polyethylene cladding.

- The detector model for 3-TeV studies is based on CLIC's detector concept + the MDI and the vertex detector designed by the US Muon Accelerator Program (MAP).
- The simulation and reconstruction software is derived from CLIC's iLCSoft (transition to the Key4hep framework in progress)
  - [github.com/MuonColliderSoft](https://github.com/MuonColliderSoft).
- The propagation of the BIB particles in the detector and their interactions with the detector materials are handled by **GEANT4**.

The following full-simulation detector studies with BIB focus on  $\sqrt{s} = 3 \text{ TeV}$ , but the findings and results also apply to the 10 TeV case because of the similarity in the BIB characteristics.

- In the tracking system, the BIB produces a **huge amount of spurious hits** (mostly from very low- $p_T$  electrons looping inside the tracker volume)
  - track finding is very challenging due due to the number of hit combinations.

charged BIB particles in the muon collider tracker (generator level)



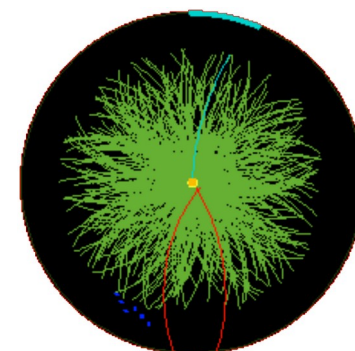
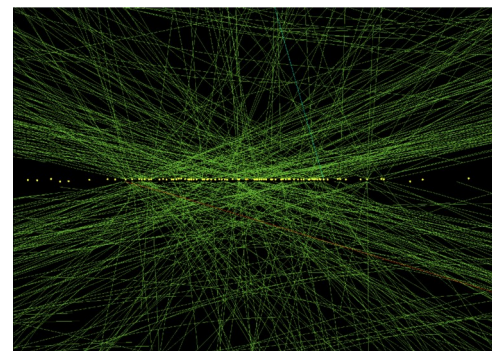
Muon Collider Detector

Detector Reference	Hit Density [ $\text{mm}^{-2}$ ]		
	MCD	ATLAS ITk	ALICE ITS3
Pixel Layer 0	3.68	0.643	0.85
Pixel Layer 1	0.51	0.022	0.51

C. Accettura et al., Eur. Phys. J. C 83 (2023) 864

Higher hit occupancies than at HL-LHC detectors are expected, but the crossing rate at the muon collider is  $\sim 30\text{-}70$  kHz vs 40 MHz at LHC.

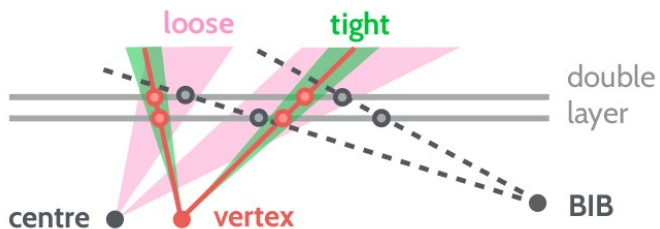
event with 78 pileup vertices at CMS



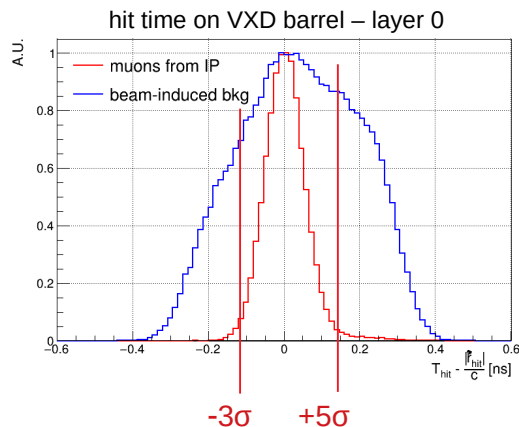
● Key features of the tracking system to deal with the BIB:

- ▶ optimized detector layout;
- ▶ high granularity;
- ▶ precise timing;
- ▶ directional information;
- ▶ characteristics of the detector response (pulse shape and pixel cluster size).

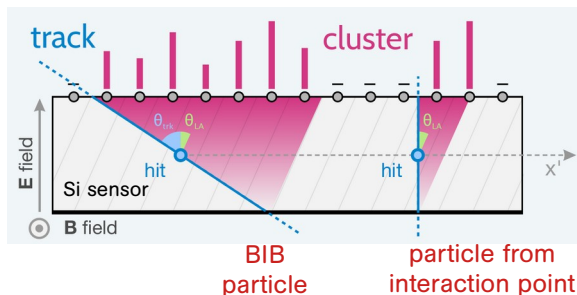
incoming direction of the particle



high-precision timing



shape and size of pixel clusters



Ongoing R&D (DRD3)

- Silicon LGAD sensors for 4D tracking up to very high fluence:
  - ▶ V. Sola et al., Nucl. Instrum. Meth. A 1040 (2022) 167232.

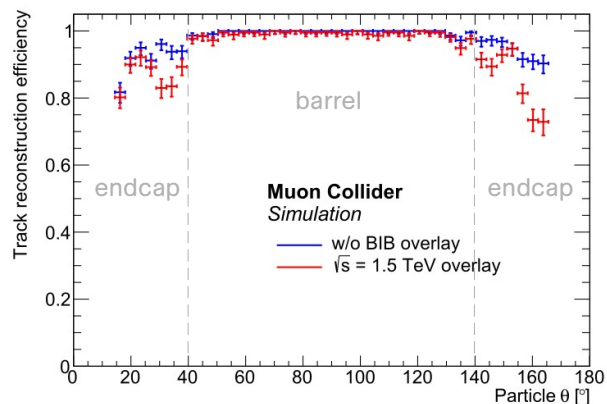
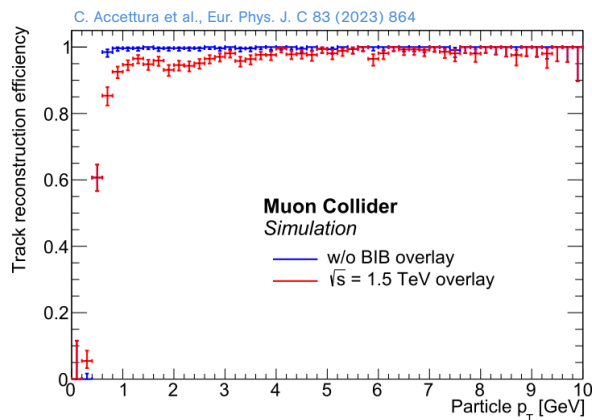


prototype with new LGAD design funded by INFN-CSN5 and AIDAInnova grants

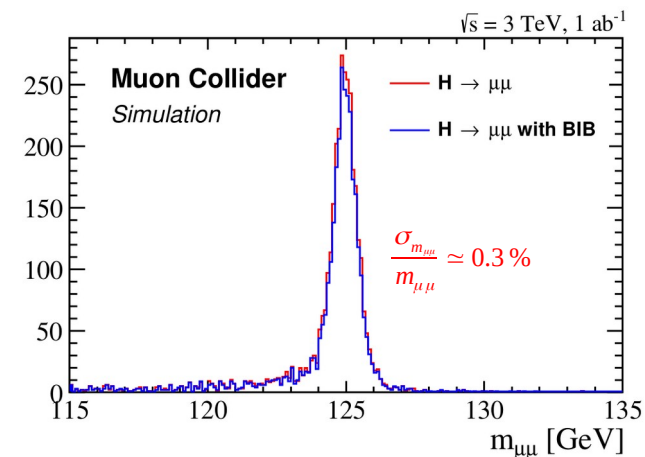
Project funded also by an EU ERC Consolidator Grant.

- In the presence of the BIB, the reconstruction algorithms for all the physics objects had to be revisited or fine-tuned.
- Detector performance assessed with **single particle samples** and **benchmark physics channels**.

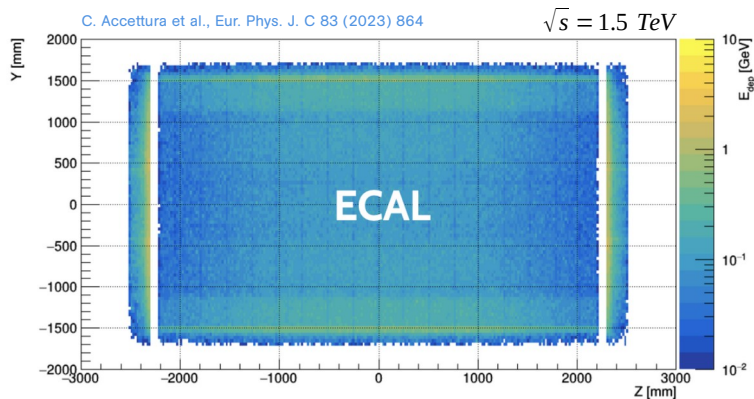
single muon samples



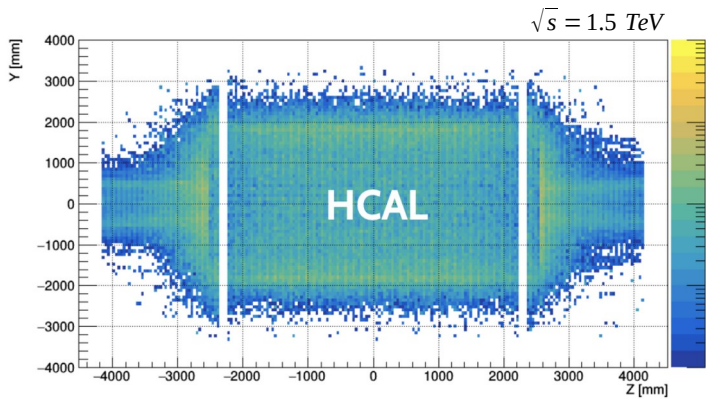
$\mu\mu \rightarrow H\nu\bar{\nu} \rightarrow \mu\mu\nu\bar{\nu}$



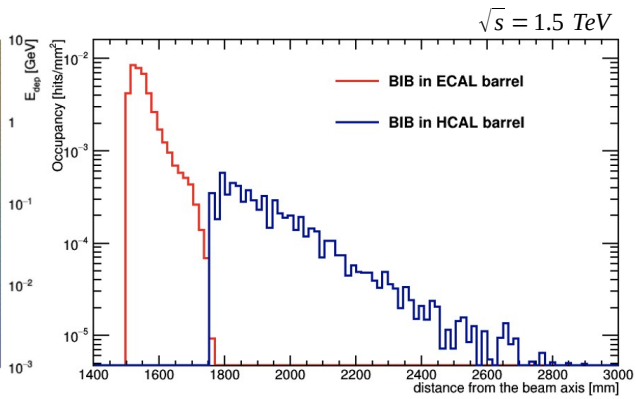
BIB energy in the electromagnetic calorimeter



BIB energy in the hadronic calorimeter



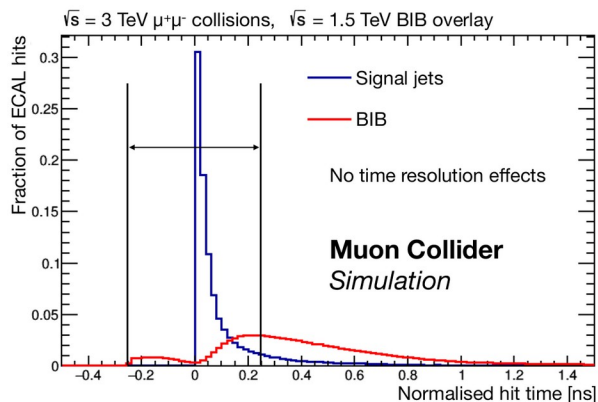
density of BIB hits vs calorimeter barrel depth



- In calorimeters, expected an **approximately uniform deposition of energy** by BIB particles.
- ECAL:
  - ▶ estimated a flux of **300 particles per cm<sup>2</sup>** through the ECAL surface at every bunch crossing;
  - ▶ **~96% photons** and **~4% neutrons**;
  - ▶ average photon energy: **1.7 MeV**.
- HCAL:
  - ▶ expected a **~10 times lower hit occupancy** due to the BIB than in the ECAL;
  - ▶ **~99% neutrons**.

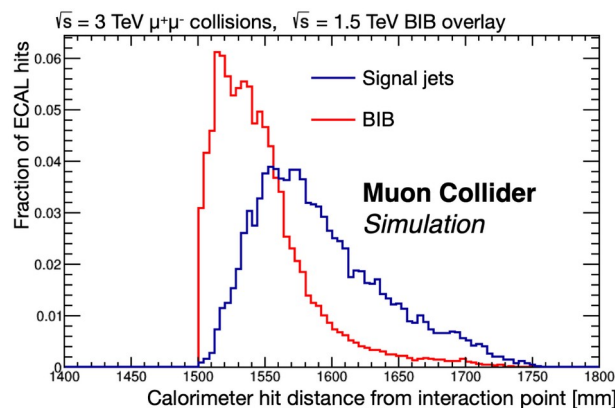
- Key calorimeter features to mitigate the BIB effects:
  - ▶ high granularity;
  - ▶ fine longitudinal segmentation;
  - ▶ resolution on the particle time of arrival of  $\sim 100$  ps.

time of ECAL barrel hits



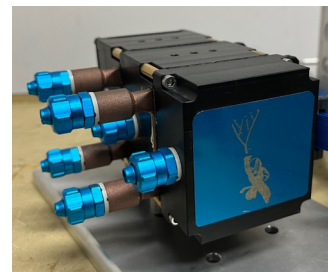
C. Accettura et al., Eur. Phys. J. C 83 (2023) 864

shower profile of signal jets vs bkg



## Ongoing R&D (DRD6)

- Semi-homogeneous electromagnetic calorimeter based on lead fluoride crystals (CRILIN):
  - ▶ S. Ceravolo et al., Nucl. Instrum. Meth. A 1047 (2023) 167817.



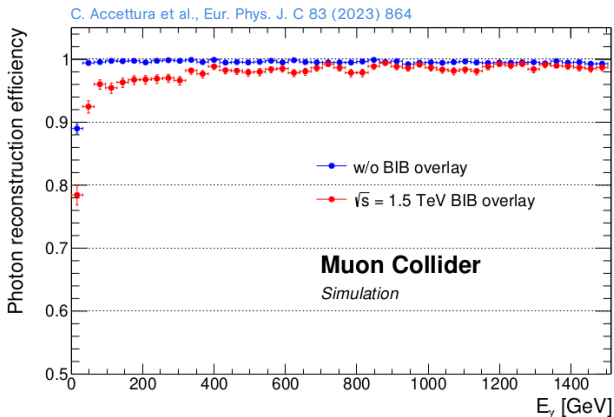
2-layer 3x3-crystal CRILIN prototype funded by INFN

- Hadronic calorimeter based on Micro-Pattern Gaseous Detectors:
  - ▶ C. Aruta et al., Nucl. Instrum. Meth. A 1047 (2023) 167731.

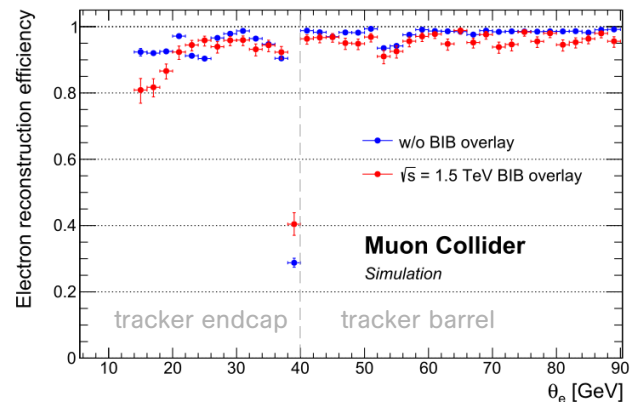
Funding from the Italian Ministry for Universities and Research (“PRIN”) to build an integrated ECAL-HCAL prototype.

# e.m. object reconstruction performance

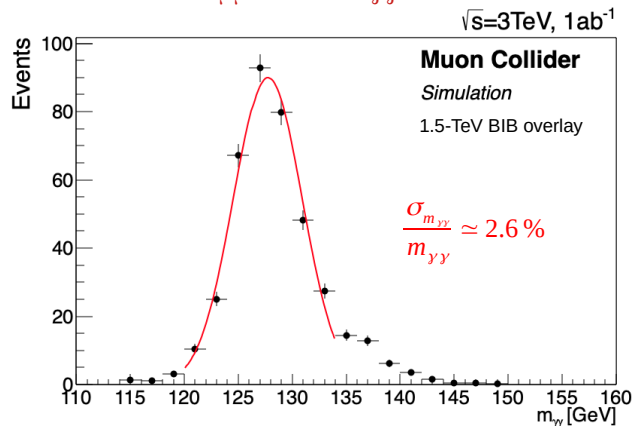
single photon sample



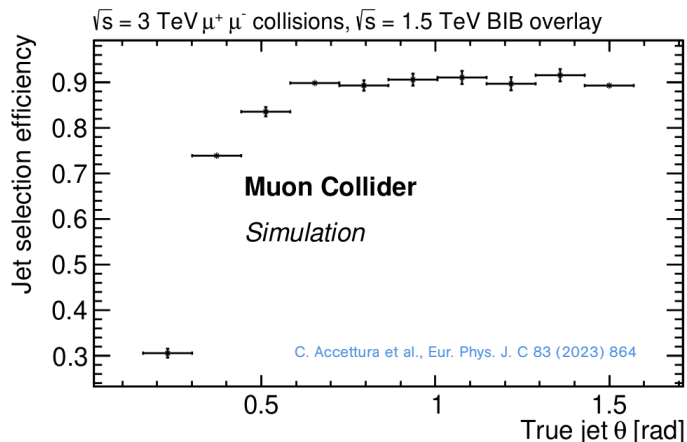
single electron sample



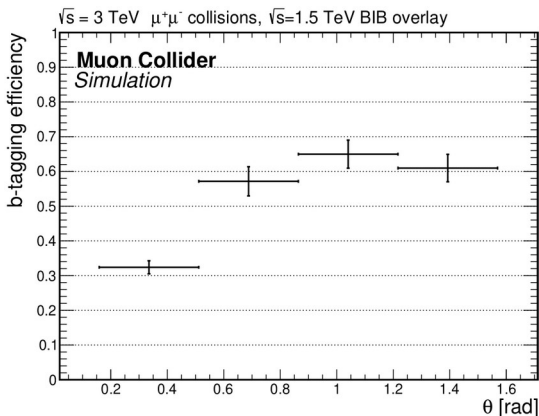
$\mu\mu \rightarrow H\nu\bar{\nu} \rightarrow \gamma\gamma\nu\bar{\nu}$



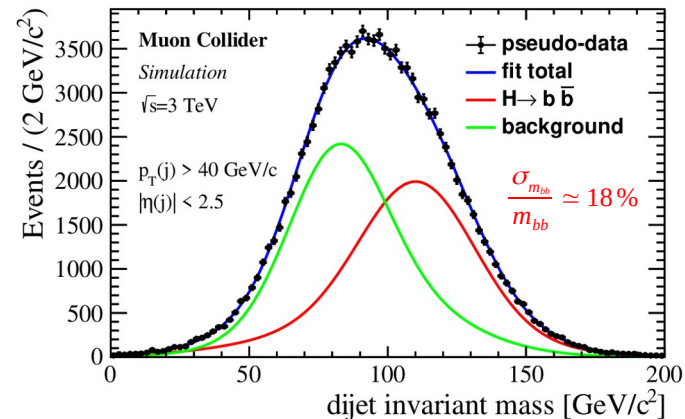
dijet samples



$b\bar{b}$  sample

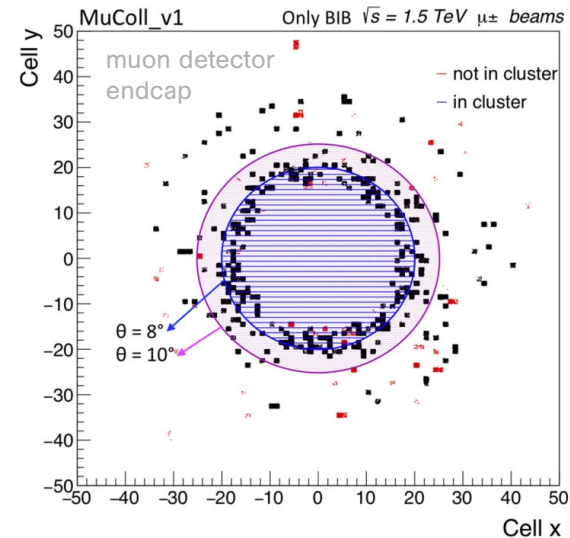
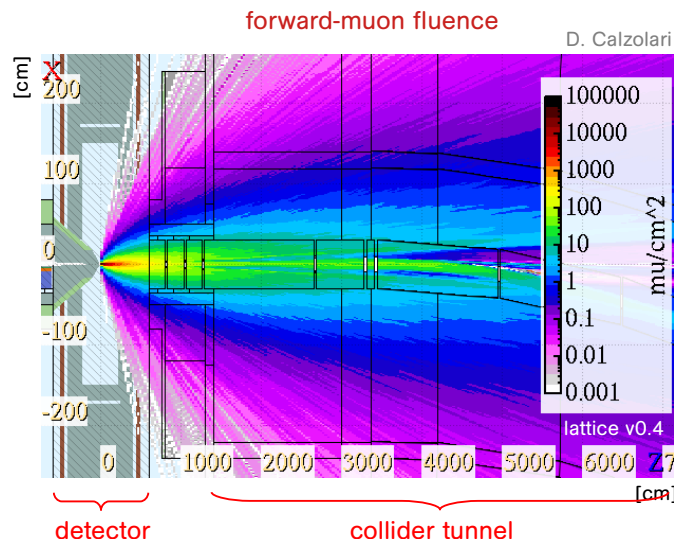
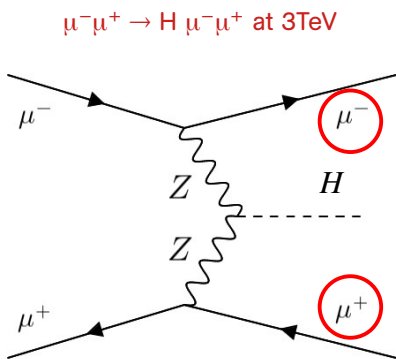


$\mu\mu \rightarrow H\nu\bar{\nu} \rightarrow b\bar{b}\nu\bar{\nu}$



- To reduce contamination from BIB hits, the energy thresholds for ECAL and HCAL hits have been set to 2 MeV.
- Despite crude background mitigation measures, simple calibration procedures, and non-optimized reconstruction algorithms, the performance of the 3 TeV detector in reconstructing the main physics objects is already satisfactory.

- In the muon system, significant BIB effects only in the endcap regions close to the beamline:
  - ▶ required good spatial resolution and possibly sub-ns time resolution.
- Under investigation the possibility of detecting the forward-scattered muons associated with the ZZ-fusion production process:
  - ▶ exploit the specific ZZ-fusion signature;
  - ▶ possibly help with the luminosity measurement.

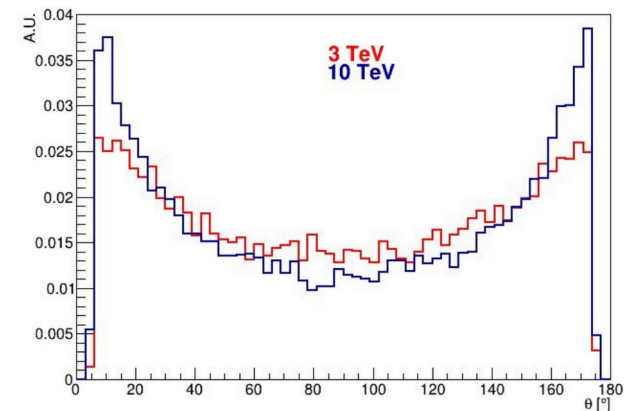
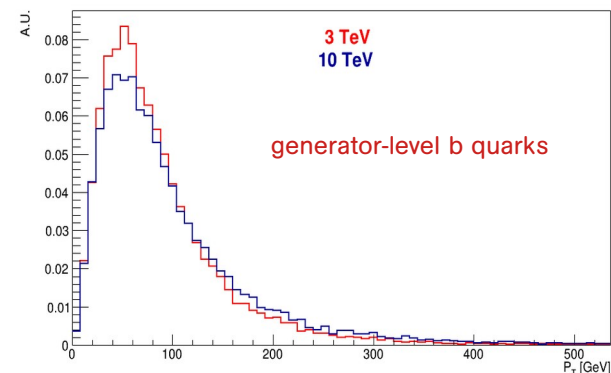


## Ongoing R&D (DRD1)

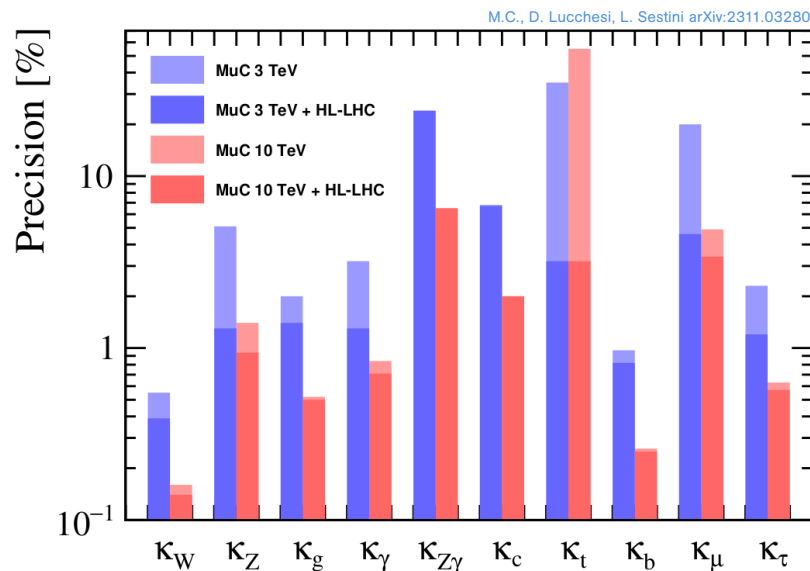
- Muon detector based on PicoSec Micromegas:
  - ▶ C. Aimè et al., 2024 JINST 19 C03052.

- Basic plan for the next update of the European Strategy for Particle Physics is to assess the detector performance on a set of **representative physics channels with a detailed detector simulation** that includes the machine background.
- Focus on benchmark processes with low- and high- $p_T$  physics objects:
  - ▶ At  $\sqrt{s} = 3$  TeV (results to be submitted to JHEP):
    - ◆ production cross sections of Higgs boson into  $b\bar{b}$ ,  $WW^*$ ,  $ZZ^*$ ,  $\gamma\gamma$ ,  $\mu\mu$ 
      - Higgs properties at 3 and 10 TeV very similar, conclusions on the detector requirements apply also for 10 TeV;
    - ◆ double Higgs production and **Higgs trilinear self-coupling** in the channel  $HH \rightarrow b\bar{b}b\bar{b}$ .
  - ▶ At  $\sqrt{s} = 10$  TeV:
    - ◆ Higgs boson **self-couplings** in as many decay channels as possible;
    - ◆ **Z' boson production**.

$\mu\mu \rightarrow H\nu\bar{\nu} \rightarrow b\bar{b}\nu\bar{\nu}$  at  $\sqrt{s} = 3$  and 10 TeV



- Higgs boson couplings to fermions and bosons are extracted from a global fit to the Higgs boson production cross sections:
  - ▶ the set of channels of full-simulation studies at 3 TeV is not yet complete for a global fit;
  - ▶ the muon collider potential at 3 TeV ( $1 \text{ ab}^{-1}$ ) and 10 TeV ( $10 \text{ ab}^{-1}$ ) is evaluated with a **parametric detector simulation** (partially tuned on the detailed detector simulation at 3 TeV) by M. Forslund and P. Meade and JHEP 08 (2022) 185.



# Higgs boson self-couplings

- A precise measurement of the Higgs boson self-couplings  $\lambda_3$  and  $\lambda_4$  would allow to constraint the shape of the Higgs potential:

$$V(h) = \frac{1}{2} m_H^2 h^2 + \lambda_3 v h^3 + \frac{1}{4} \lambda_4 h^4$$

- **At 3 TeV** sensitivity study with **full simulation** on  $\lambda_3$  using the channel  $\mu\mu \rightarrow HH\nu\bar{\nu} \rightarrow b\bar{b}b\bar{b}\nu\bar{\nu}$ :

$$\frac{\Delta \lambda_3}{\lambda_3} \sim 20-30\% \quad (1 \text{ ab}^{-1} \text{ with 1 experiment})$$

CLIC at 3 TeV with 2  $\text{ab}^{-1}$  and  $e^-$  beam polarization ( $b\bar{b}b\bar{b} + \bar{b}bWW^* \rightarrow \bar{b}b\bar{q}q'\bar{q}q'$ ): 22%

H. Abramowicz et al., Eur. Phys. J. C 77, 475 (2017)

- ▶ in line with a parametric study by T. Han et al., Phys. Rev. D 103 (2021) 013002:

$$\frac{\Delta \lambda_3}{\lambda_3} = 25\% \quad (1 \text{ ab}^{-1} \text{ with 1 experiment}).$$

- But the full potential of the muon collider emerges at higher energies:

- ▶ **at 10 TeV** the same parametric study by T. Han et al. estimates:

$$\frac{\Delta \lambda_3}{\lambda_3} = 5.6\% \quad (10 \text{ ab}^{-1} \text{ with 1 experiment}).$$

## Quartic self-coupling

- Phenomenological study by M. Chiesa et al., JHEP 09 (2020) 098:

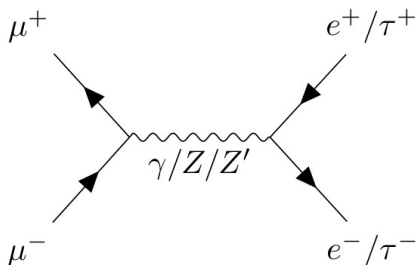
- ▶ at 10 TeV assuming 20  $\text{ab}^{-1}$ :

$$\Delta\lambda_4/\lambda_4 \sim 50\%.$$

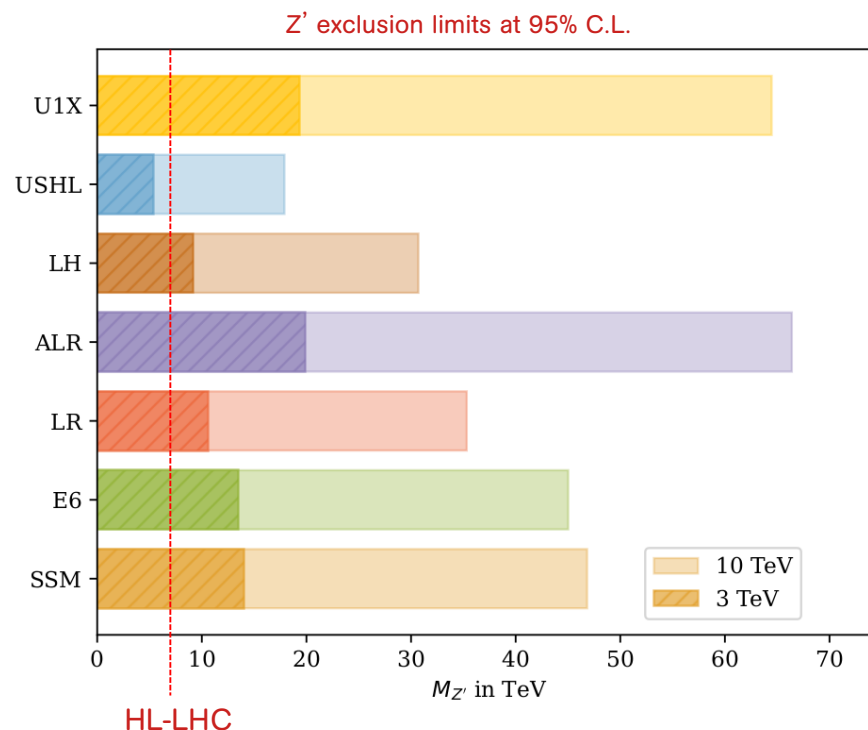
# Example of Z' searches

- New Z' bosons can be probed directly up to  $M_{Z'} \sim \sqrt{s}$ , but indirect searches extend much beyond:
  - ▶ example of a phenomenological study exploring the reach of a muon collider for additional neutral gauge bosons that couple to the standard model: K. Korshynska et al., arXiv:2402.18460.

- Indirect discovery potential for a new Z' boson coupled to the standard model in the final states ee and  $\tau\tau$ :



- ▶ assumed  $1 \text{ ab}^{-1}$  at  $\sqrt{s} = 3 \text{ TeV}$  and  $10 \text{ ab}^{-1}$  at  $\sqrt{s} = 10 \text{ TeV}$ ;
- ▶ off-peak analysis based on observables of the final state leptons.

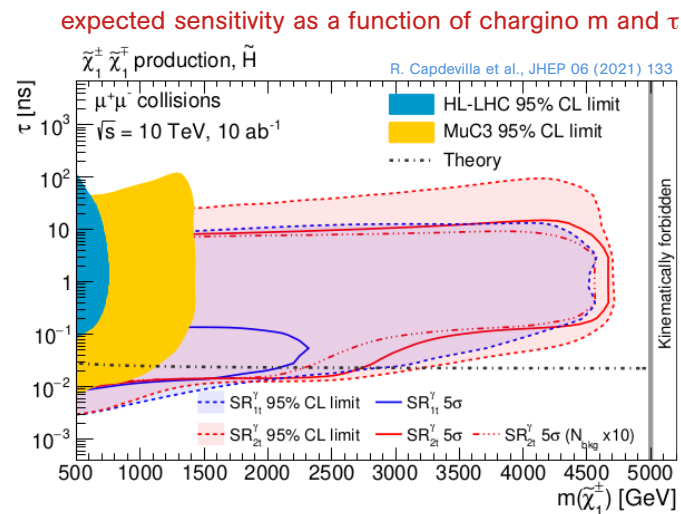
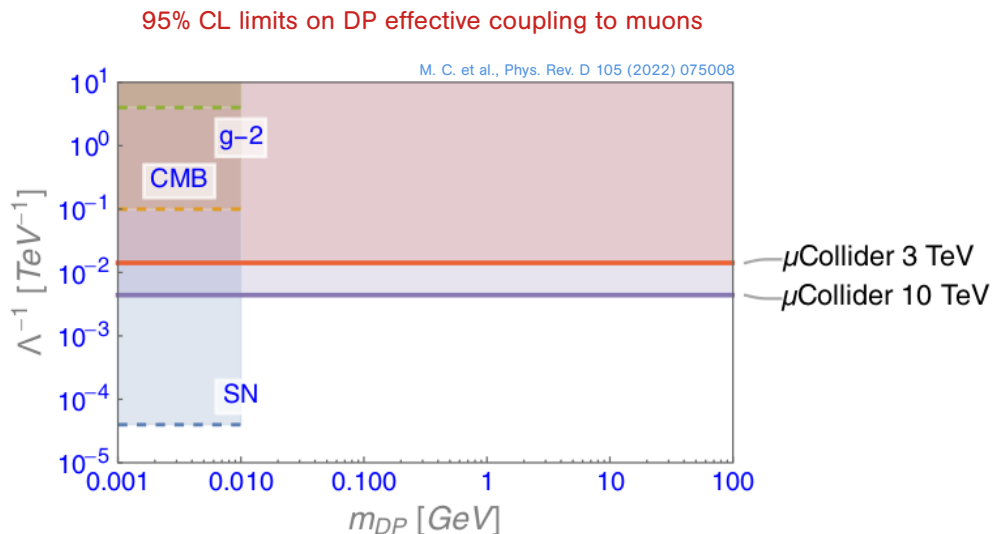


# Example of dark matter searches

● Higgs boson couplings represent a guaranteed result, but the muon collider physics program is much broader.

▶ Search for a dark photon (DP) or an ALP produced in association with a photon at  $\sqrt{s} = 3 \text{ TeV}$  ( $1 \text{ ab}^{-1}$ ) and  $\sqrt{s} = 10 \text{ TeV}$  ( $10 \text{ ab}^{-1}$ ) in events with a **single monochromatic photon**.

▶ Search for wino and higgsino dark matter at  $\sqrt{s} = 3 \text{ TeV}$  ( $1 \text{ ab}^{-1}$ ) and  $\sqrt{s} = 10 \text{ TeV}$  ( $10 \text{ ab}^{-1}$ ) with the **disappearing track signature**.



# Detector concepts for 10 TeV collisions

- Two detector concepts are currently under development with different layouts.
  - ▶ key features being optimized: tracker radius, magnetic field intensity, calorimeter depth.

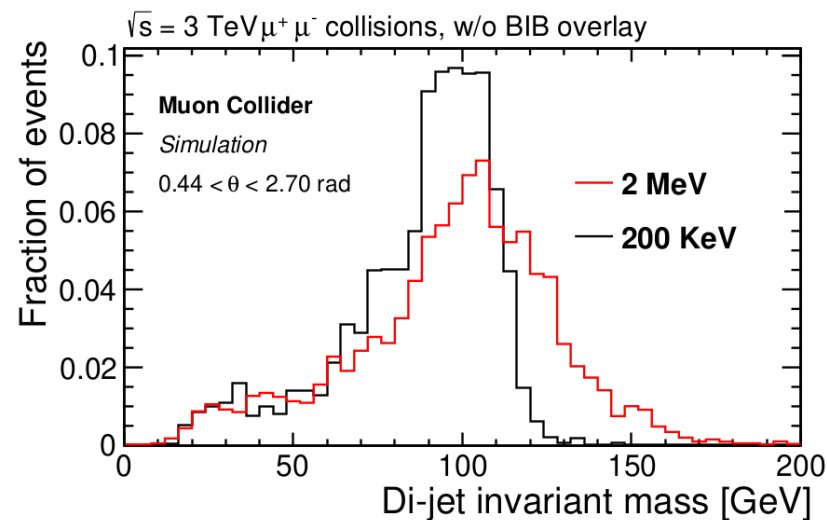
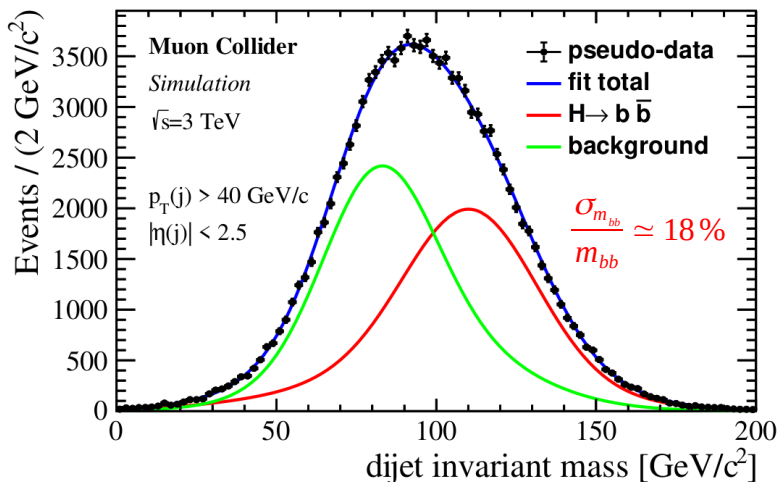


- The effects of **beam-induced background** in the detector have been thoroughly studied with a detailed detector simulation and mitigation measures are in place to keep them **under control**.
- **Full-simulation studies at 3 TeV** are concluded and results will be **soon published**.
- The full-simulation studies point the way for the **detector R&D** (some R&D's already well advanced).
- The goals for the **European Strategy update** are a **detector concept for 10 TeV collisions** and the **muon collider reach for representative physics cases**.

**Backup**

# $b\bar{b}$ mass resolution vs hit energy threshold

$$\mu\mu \rightarrow H\nu\bar{\nu} \rightarrow b\bar{b}\nu\bar{\nu}$$



- Hadronic jets are reconstructed using also low-energy objects: the energy threshold of 2 MeV for the calorimeter hits affects the energy resolution.

# Full sim vs parametric sim at 3 TeV

		Full sim		Fast sim	
Cross sections resolution	→	H->WW	2.9%	H->WW	1.7%
		H->ZZ	17%	H->ZZ	11%
		H->bb	0.75%	H->bb	0.76%
		H-> $\mu\mu$	38%	H-> $\mu\mu$	40%
		H-> $\gamma\gamma$	8.9%	H-> $\gamma\gamma$	6.1%
		HH->4b	30%		
Couplings resolution	→	$g_{HWW}$	0.9%	$g_{HWW}$	0.55%
		$g_{HZZ}$	8.2%	$g_{HZZ}$	5.1%
		$g_{Hbb}$	0.8%	$g_{Hbb}$	0.97%
		$g_{H\mu\mu}$	19%	$g_{H\mu\mu}$	20%
		$g_{H\gamma\gamma}$	4.5%	$g_{H\gamma\gamma}$	3.2%
		$\lambda_3$	20%	$\lambda_3$ (95% CL)	25%

M. Forsslund and P. Meade and JHEP 08 (2022) 185

S. Dawson et al., Report of the Topical Group on Higgs Physics for Snowmass 2021: The Case for Precision Higgs Physics, arXiv:2209.07510

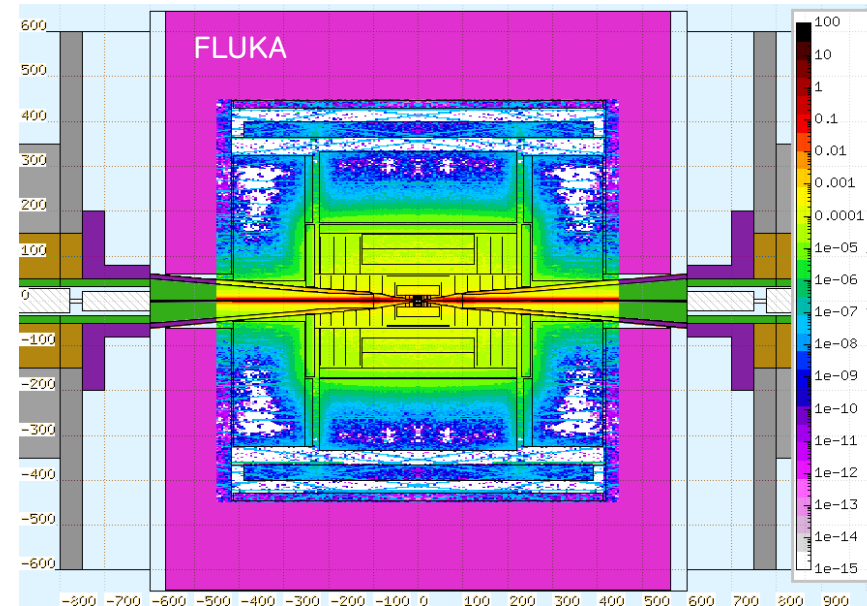
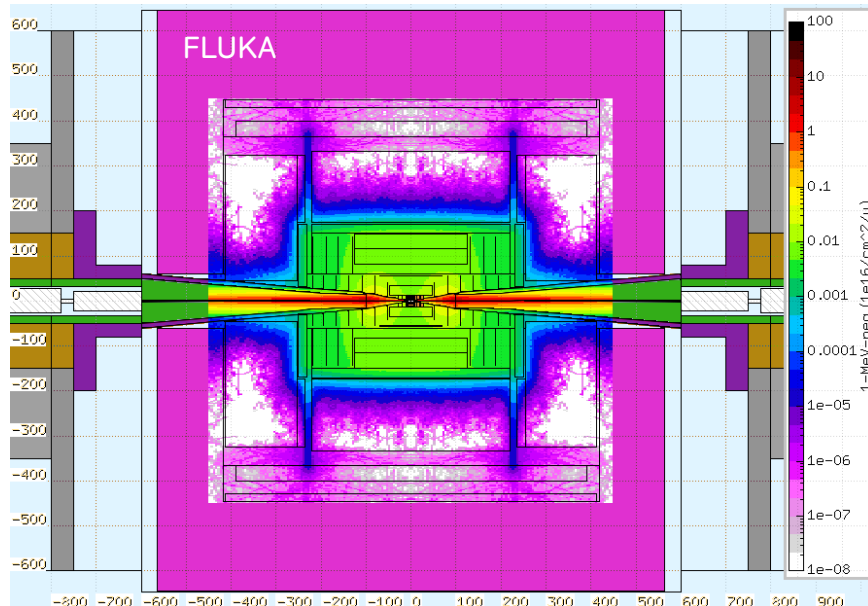
Higgs Coupling (%)	HL-LHC	ILC250 + HL-LHC	ILC500 + HL-LHC	ILC1000 + HL-LHC	FCC-ee + HL-LHC	CEPC240 + HL-LHC	CEPC360 + HL-LHC	CLIC380 + HL-LHC	CLIC3000 + HL-LHC	$\mu(10\text{TeV})$ + HL-LHC	$\mu 125$ + HL-LHC	FCC-hh + FCCee/FCCeh
$hZZ$	1.5	.22	.17	.16	.17	.074	.072	.34	.22	.33	1.3	.12
$hWW$	1.7	.98	.20	.13	.41	.73	.41	.62	1	.1	1.3	.14
$hb\bar{b}$	3.7	1.06	.50	.41	.64	.73	.44	.98	.36	.23	1.6	.43
$h\tau^+\tau^-$	3.4	1.03	.58	.48	.66	.77	.49	1.26	.74	.55	1.4	.44
$hgg$	2.5	1.32	.82	.59	.89	.86	.61	1.36	.78	.44	1.7	.49
$hc\bar{c}$	-	1.95	1.22	.87	1.3	1.3	1.1	3.95	1.37	1.8	12	.95
$h\gamma\gamma$	1.8	1.36	1.22	1.07	1.3	1.68	1.5	1.37	1.13	.71	1.6	.29
$h\gamma Z$	9.8	10.2	10.2	10.2	10	4.28	4.17	10.26	5.67	5.5	9.8	.69
$h\mu^+\mu^-$	4.3	4.14	3.9	3.53	3.9	3.3	3.2	4.36	3.47	2.5	.6	.41
$ht\bar{t}$	3.4	3.12	2.82	1.4	3.1	3.1	3.1	3.14	2.01	3.2	3.4	1.0
$\Gamma_{tot}$	5.3	1.8	.63	.45	1.1	1.65	1.1	1.44	.41	.5	2.7	

S. Dawson et al., Report of the Topical Group on Higgs Physics for Snowmass 2021: The Case for Precision Higgs Physics, arXiv:2209.07510

collider	Indirect- $h$	$hh$	combined
HL-LHC [78]	100-200%	50%	50%
ILC <sub>250</sub> /C <sup>3</sup> -250 [51, 52]	49%	–	49%
ILC <sub>500</sub> /C <sup>3</sup> -550 [51, 52]	38%	20%	20%
CLIC <sub>380</sub> [54]	50%	–	50%
CLIC <sub>1500</sub> [54]	49%	36%	29%
CLIC <sub>3000</sub> [54]	49%	9%	9%
FCC-ee [55]	33%	–	33%
FCC-ee (4 IPs) [55]	24%	–	24%
FCC-hh [79]	-	3.4-7.8%	3.4-7.8%
$\mu$ (3 TeV) [64]	-	15-30%	15-30%
$\mu$ (10 TeV) [64]	-	4%	4%

1-MeV neutron equivalent fluence per year

total ionizing dose per year



**Assumptions:**

- ◆ collision energy: 1.5 TeV;
- ◆ collider circumference: 2.5 km;
- ◆ beam injection frequency: 5 Hz;
- ◆ days of operation per year: 200.

	Maximum Dose (Mrad)		Maximum Fluence ( $1\text{ MeV-neq/cm}^2$ )	
	R= 22 mm	R= 1500 mm	R= 22 mm	R= 1500 mm
Muon Collider	10	0.1	$10^{15}$	$10^{14}$
HL-LHC	100	0.1	$10^{15}$	$10^{13}$

Radiation hardness requirements are similar to what expected at HL-LHC.